



# DEM Generation from High Resolution Satellite Imagery

KARSTEN JACOBSEN, Hannover

**Keywords:** digital elevation models, satellite imagery, image matching, accuracy

**Summary:** Digital height models (DHM) covering larger areas can be generated by means of optical or synthetic aperture radar (SAR) images taken from space. An overview of the sensors and the characteristics of generated height models is given. With very high resolution optical satellite stereo pairs a system accuracy of 1.0 ground sampling distance (GSD) standard deviation can be reached. Of course this is not the accuracy of a DEM, which is also influenced by interpolation and includes areas with limited contrast and vegetation, leading to lower quality. In addition, the difference between digital surface models (DSMs), describing the visible surface, and digital terrain models (DTMs), describing the bare ground, has to be respected. The same problem exists for SAR images used by either interferometric SAR (InSAR) or by radargrammetry if no InSAR configuration is available. It has to be ascertained whether existing regional or nearly worldwide DEMs can be used instead of especially produced elevation models. The SRTM DEM and ASTER GDEM are both available, free of charge via the Internet, but their resolution and accuracy are limited. Higher resolution DEMs, such as the SPOT DEM (also named Reference 3D) or Next-Map, are not free of charge and they do not cover the whole earth. This will also be the case for the TanDEM-X height model, which will be available in 2014. If more detailed DEMs are required, they can be determined by automatic image matching of very high resolution satellite imagery.

**Zusammenfassung:** Erzeugung von Höhenmodellen aus hochauflösten Satellitenbildern. Digitale Höhenmodelle, die eine größere Fläche erfassen, können mittels optischer oder Radar-Weltraumbilder erstellt werden. Es wird ein Überblick über die Sensoren und die Charakteristik der erstellten Höhenmodelle gegeben. Mit sehr hoch auflösenden optischen Satellitenbildstereopaaren kann eine Systemgenauigkeit von etwa 1,0 Bodenpixelgröße erreicht werden. Die Systemgenauigkeit ist nicht die Genauigkeit eines DHM, das durch Bereiche mit niedrigerem Kontrast, Interpolation und Vegetation beeinflusst sein kann. Zusätzlich sind die erzeugten digitalen Oberflächenmodelle nicht identisch mit einem DHM, das die Höhe des Erdbodens beschreibt. Das gleiche Problem existiert für die mittels Interferometrischem Radar oder Radargrammetrie erstellten Höhenmodelle. Bevor Höhenmodelle erstellt werden, sollte überprüft werden, ob nicht auch vorhandene weltweite oder regionale Höhenmodelle benutzt werden können. Nahezu weltweite Höhenmodelle wie das SRTM DHM und ASTER GDEM sind heute kostenlos verfügbar. Ihre Auflösung und Genauigkeit ist begrenzt. Verfügbare höher auflösende DHM wie Reference 3D oder NextMap sind nicht kostenlos. Dieses wird auch für das TanDEM-X Global DEM gelten, das in der Basisversion 2014 über ASTRIUM vertrieben wird. Werden detailliertere Höhenmodelle benötigt, können sie mittels sehr hoch auflösender optischer Stereobildpaare erstellt werden.

## 1 Introduction

Traditionally, height models have been based on aerial images. With the improved resolution of optical and radar satellites, space images provide a range of ground resolutions which overlap the resolution range of aerial images, so it is a question of economy and access to aerial imagery that dictates which

source should be used to generate a height model. Nearly worldwide height models, or at least those covering large areas, are generally based on data from space-borne platforms because of limited access to aerial imagery. For local areas as well, it is sometimes more economic to use space images instead of organizing a photo flight. Digital height models (DHM) can be generated with optical stereo

pairs or even tri-stereo models, with synthetic aperture radar (SAR) image pairs by interferometric SAR (InSAR) or by radargrammetry. Before DHMs meeting specified requirements are acquired, it should be checked if they are available free of charge. A DHM can be characterized by its accuracy, resolution and the vertical location of its points. Usually, digital surface models (DSM) with points located on the visible surface are initially generated. Only with L- and P-band radar can the vegetation be penetrated so as to directly produce DEMs with 'bare-ground' points with the exception of points coinciding with buildings. In all other cases, DEMs have to be generated by filtering and manual post processing. Morphological characteristics partially dictate the point spacing, i.e. the resolution of the DHM. Resolution is influenced by the roughness of the terrain, and in the case of data fusion, surface detail can be lost if the merged DHMs are not accurately registered in planimetry.

## 2 Accuracy Figures

Accuracy figures are related to data with normally distributed height discrepancies, usually computed in relation to reference height models with at least the same accuracy as the investigated DHM. Normally distributed discrepancies are based on a presupposed optimal fitting together of the DHMs, which implies the absence of shifts in X, Y and Z. Horizontal shifts between height models are common and they can be caused by orientation and datum problems. A check for such shifts is required before analysis of the accuracy of DHMs. The adjustment of the height model fitting is based on the height differences and the terrain inclination ( $DX = Dh / \tan(\text{inclination } X)$ ), where DX is an unknown shift and Dh is the height difference to the reference DHM):

$$SZ = \sqrt{\frac{\sum (v - m)^2}{n - u}} \quad (1)$$

Here, SZ is the standard deviation of Z, v is the height discrepancy, m the mean, n the number of observations and u the number of unknowns. Also, the median absolute deviation (MAD) is given as

$$MAD = \text{median of } |v| \quad (2)$$

and the normalized median absolute deviation (NMAD) as

$$NMAD = MAD * 1.4815 \quad (3)$$

Moreover,

LE90 = linear error, 90% probability (threshold value); for a normal distribution  $LE90 = SZ * 1.65$

LE95 = linear error, 95% probability (threshold value); for a normal distribution  $LE95 = SZ * 1.96$

CE90 = circular error, 90% probability (threshold value); for a normal distribution and equal standard deviation values in X and Y,  $CE90 = SX * 2.146$

In the case of normally distributed observations, SZ is identical to NMAD, both having a probability value of 68%. If the observations are not normally distributed, generally because of the presence of large discrepancies, SZ will be larger than NMAD because SZ is more influenced by large discrepancies. A normal distribution requires the same condition for all observations and this usually is not the case for the heights of a DHM. At first we have a dependency upon the terrain inclination, which can be appreciated, but in the case of matching optical images, we may also have different object contrast. Or, in the case of SAR, we may have problems with foreshortening, total reflection by water surfaces or poor back scatter in dry sand deserts. These different conditions can be included in an error map, but not all height models have such error maps. Thus, there can be shortcomings in the assumption of normally distributed height discrepancy values, especially if a DSM is compared with a DEM. Of course it is not correct to compare a DSM to a DEM; this causes asymmetric deformation of the frequency distribution. The influence of vegetation and buildings cannot be handled as a standard deviation. In such a case the investigation should be carried out within just the open bare ground areas, not including trees and buildings. However, open areas may also have individual trees or buildings, requiring a filtering for objects not belonging to the bare earth (PASSINI et al. 2002, DAY et al. 2013).

### 3 High and Very High Resolution Optical Satellites

Today, approximately 15 satellites with very high resolution (VHR) optical systems, of 1 m ground sampling distance (GSD) or better, provide imagery for civilian use. The theoretical imaging capacity per day for this whole group of optical satellites is approximately 20 times higher than for IKONOS and QuickBird together. Nevertheless, even with this many VHR optical satellites the goal of close to worldwide coverage with stereo models is unrealistic. Coverage of such an extensive geographic area is only feasible with lower resolution stereo satellites such as SPOT 5 HRS with 5 m GSD in flight direction, Cartosat-1

with 2.5 m GSD, Ziyuan 3 with 3.2 m GSD, or ASTER with 15 m GSD. Even so, several years of data acquisition from these sensors are required for near-global DEM coverage.

Height models should be based on stereo pairs with images taken at approximately the same time. This requires a fast and agile satellite rotation if the images are to be recorded within the same orbit, within approximately 1 minute. The matching of images having larger time differences invariably causes problems due to variations of object illumination and changes in shadows. QuickBird needs approximately 50 s for a rotation of 35°, so the stereo pair alone can be recorded within a single orbit covering a given local area of interest. The stereo imaging coverage per pass is

**Tab. 1:** Optical satellites able to generate stereo pairs from the same orbit by rotating the satellite. The values surrounded by brackets, e.g. (0.41), show the physical resolution while for legal reasons the finest resolution is restricted to 0.50 m.

Satellite	Launch	GSD pan (m)	GSD ms (m)	Swath in nadir (km)	Flying height (km)
IKONOS	1999	0.81	3.24	16.5	680
QuickBird	2001	0.62	2.48	16.5	450
Formosat-2	2004	2	8	24	888
Kompsat 2	2006	1	4	15	685
Cartosat-2	2007	1	-	10	635
WorldView-1	2007	0.5	-	17.6	496
GeoEye-1	2008	(0.41)	(1.65)	15.2	684
THEOS	2008	2	15	22	822
Cartosat-2A	2008	1	-	10	635
WorldView-2	2009	(0.46)	(1.84)	16.4	770
Cartosat-2B	2010	1	-	10	635
Pleiades 1B	2011/12	0.7	2.8	51.1	506
Kompsat-3	2012	0.7	2.8	15	685
SPOT-6	2012	2.0	8.0	60	694
planned					
Kompsat-3A	2013	0.7	2.8	15	685
GeoEye-2	2013	(0.34)	(1.36)	14.5	681
WorldView-3	2014	(0.31)	(1.24)	13.1	617
Cartosat-3	2014	0.33	-	21	600
DMC-3 (3 satellites)	2014	1	4	22.6	630
SPOT-7	2014	2.0	8.0	60	694

better for IKONOS and GeoEye-1, requiring only 28 s. It is even more favourable for Pleiades with their approximate 18 s for rotation to capture a stereo image pair, and it is currently optimal for WorldView, which requires approximately 10 s. The sensors with more rapid rotation can take additional images along with a stereo pair, or more than one stereo pair in the same orbit, thus making them more economical.

As shown in Tab. 1, a higher number of today's optical satellites can take stereo pairs from the same orbit. For precise georeferencing, ground control points (GCP) have to be used. The number of GCPs can be reduced for a block of images by block adjustment, but GCPs may not always be available.

Tab. 2 shows the specified accuracy of direct georeferencing, which employs only the recorded sensor orientation. Whereas direct georeferencing may prove satisfactory for a given stereo model application, especially

for WorldView-1, -2, GeoEye-1 and Pleiades 1B, for other satellites the sensor orientation warrants improvement by relative orientation before computation of a stereo model and a subsequent fit of this stereo model to a reference DHM such as the SRTM DEM. With this method, Euromap generates the EURO-MAPS 3D from Cartosat-1 stereo imagery to a location accuracy of  $CE90 = 15$  m, corresponding to  $SX = SY = 7$  m.

The choice of orientation model for a scene of space images is today dominated by bias corrected rational polynomial coefficients (RPC). The RPCs are delivered together with the images and usually have only to be corrected by shift values (bias correction). In some cases correction via a 2D affine transformation is required, but this is indicated by discrepancies at GCPs. With geometric reconstruction, the same accuracy is reached as with bias corrected RPC. Approximate models such as the 3D-affine transformation or

**Tab. 2:** Specified accuracy of direct sensor orientation.

Sensor	SX = SY	CE90
IKONOS	7 m	15 m
QuickBird	9 m	23 m
Orbview-3	12 m	25 m
WorldView-1	2 m	5 m
WorldView-2	2 m	5 m
GeoEye-1	2 m	5 m
Pleiades 1B	2 m	3 m
Cartosat-1 / with in-flight calibration	200 m / 30 m	(Euromap CE90 = 15 m)
KOMPSAT-2	37 m	80 m

**Tab. 3:** Accuracy of stereo scene orientation determined with independent check points.

	SX, SY	SZ	GSD	SX, SY	SZ
SPOT-3	8.4 m	4.1 m	10 m	0.8 GSD	0.4 GSD
MOMS	3.5 m	4.5 m	4.5 m	0.8 GSD	1.0 GSD
Cartosat-1	1.5 m	2.5 m	2.5 m	0.6 GSD	1.0 GSD
IKONOS	1.0 m	1.7 m	1 m	0.7 GSD	1.7 GSD
ASTER	10.8 m	14.6 m	15 m	0.7 GSD	1.0 GSD
GeoEye-1	0.3 m	0.5 m	0.5 m	0.6 GSD	1.0 GSD
WorldView-2	0.5 m	0.3 m	0.5 m	1.0 GSD	0.6 GSD

direct linear transformation (DLT) should be avoided, especially since they require more well distributed 3D GCPs and generally have limited accuracy in mountainous areas.

Tab. 3 demonstrates the object point accuracy of satellite stereo pairs based on geometric reconstruction and bias corrected RPCs. Irrespective of the GSD value, the standard deviations SX and SY are usually below 1.0 GSD, and in the range of 1.0 GSD for SZ. Of course, this is the system accuracy at well defined object points and not the anticipated accuracy of a DSM determined by automatic image matching. A DEM is influenced by areas with low contrast, vegetation, buildings and terrain roughness.

Fig. 1 shows a quality image, which indicates the range of correlation coefficient values obtained in an area-based least squares

matching adjustment. The figure highlights the uniformly high correlation coefficient values found in open areas, and the lower values in forests where the image matching is not as good. Failure for water bodies is also indicated. A threshold for the correlation coefficients of 0.6 would eliminate 8% of the matched points. This can be accepted because such areas can also be interpolated from the neighbourhood. Pixel-based matching, such as semi-global matching (SGM) (HIRSCHMÜLLER 2005), has no advantage in such an area, with its high percentage of forest. However, this is different in mountainous and build up areas (ALBEID et al. 2011), where pixel-based matching can more precisely determine edges and thus allow a point spacing of one or two GSD, as opposed to area-based matching

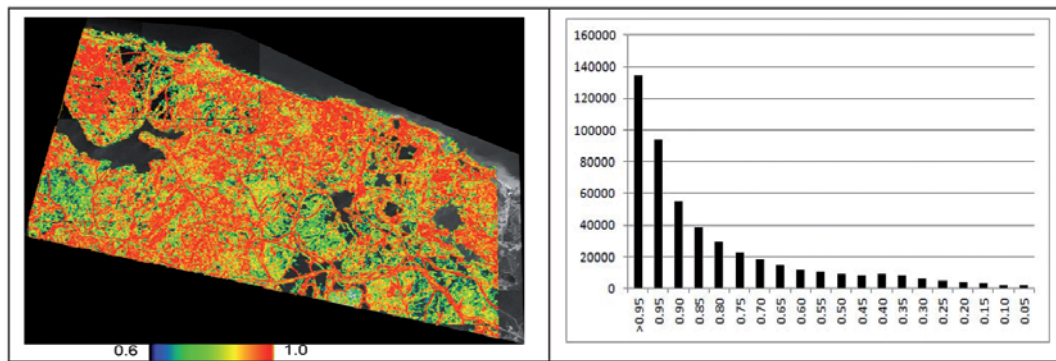


**Fig. 1:** Left: quality image of WorldView-2 image matching (size of correlation coefficient), Black Sea coast close to Istanbul, right: frequency distribution of correlation coefficients ~ 8% below the threshold of  $r = 0.6$  – dominantly located in forested areas.

**Tab. 4:** Accuracy analysis of WorldView-2 DSM Istanbul, absolute accuracy and as function of the terrain inclination with the slope  $\alpha$ .

	SZ	NMAD
WV-2 DSM against WV-2 DSM, open area	0.86 m $0.66 \text{ m} + 1.79 \text{ m} \cdot \tan\alpha$	0.69 m $0.50 \text{ m} + 1.29 \text{ m} \cdot \tan\alpha$
WV-2 DSM against reference DTM	3.65 m $3.25 \text{ m} + 5.58 \text{ m} \cdot \tan\alpha$	2.23 m $2.05 \text{ m} + 5.17 \text{ m} \cdot \tan\alpha$
WV2 DSM against reference DTM, open areas without quarries	2.21 m $1.85 \text{ m} + 3.93 \text{ m} \cdot \tan\alpha$	1.72 m $1.28 \text{ m} + 3.24 \text{ m} \cdot \tan\alpha$
WV-2 DSM against laser DSM	3.12 m $3.12 \text{ m} + 0.0 \text{ m} \cdot \tan\alpha$	1.40 m $1.40 \text{ m} + 0.0 \text{ m} \cdot \tan\alpha$
WV-2 DSM against laser DSM, open areas without quarries	1.05 m $0.83 \text{ m} + 2.28 \text{ m} \cdot \tan\alpha$	0.71 m $0.62 \text{ m} + 1.96 \text{ m} \cdot \tan\alpha$

where the minimum point spacing of the generated DHM is generally three GSD.

The area shown in Fig. 1 overlaps with an independent WorldView-2 stereo pair, which was recorded in the same orbit. The corresponding height model is based on different GCPs than the first DHM, allowing a comparison between both (Tab. 4). In addition, the DHM has been compared with a reference DEM from the Turkish survey administration. The presence of both vegetation and severe terrain height changes in quarries adversely influences the accuracy estimation, as also illustrated in the analysis restricted to open areas only, not influenced by quarries. In addition, a laser scanning DSM was used as reference surface model (Tab. 4). Because of datum problems all DHM have been shifted by adjustment to the same vertical and horizontal datum.

As usual, the influence of the terrain inclination is obvious in this partially mountainous area. The Koppe formula  $SZ = A + B \cdot \tan(\text{terrain slope})$  generally fits well with the accuracy determined for different terrain slope classes. In the open areas, corresponding for flat terrain, the two independent WorldView-2 DSMs agree to a standard deviation for a single DSM of  $0.66 \text{ m} / 1.414 = 0.47 \text{ m}$ , or with a NMAD of 0.35 m, which is below 1.0 GSD. Against the reference DEM, the difference is larger because of the limited accuracy of the reference model. In addition, it is important here to also analyse the bare open areas that exclude the quarries, so as to avoid the influence of vegetation and steep slopes. The difference between the WorldView-2 DSM and

the lidar DSM amounted to  $SZ = 1.05 \text{ m}$ , with a smaller resulting value for NMAD of 0.71 m. Nevertheless, the definition of the surface via the laser beam is different to that derived via image matching, especially given that the low vegetation undergoes seasonal variation.

The frequency distributions in Fig. 2 are typical. If the whole area without any separation is analyzed together, the frequency function is asymmetric and shows a higher number of larger discrepancies than the normal distribution, due to the inclusion of forest and changed quarry areas. The normal distribution related to NMAD fits better to the determined frequency function than the normal distribution based on SZ. The frequency function limited to the open areas (right hand side of Fig. 2) shows a better approximation to the normal distribution based on SZ than is the case for the whole area, but here also the normal distribution based on the NMAD better describes the real frequency function. This can be shown for nearly all height models, independent of the data source. The comparison of the two WorldView-2 DSMs indicate a system accuracy of  $SZ = 1.0 \text{ GSD}$  or even slightly better. A similar system accuracy is also achieved with nearly all optical satellite stereo pairs. But the system accuracy is not the accuracy of a height model; at first the influence of trees and buildings has to be respected and areas with lower image contrast cannot be avoided. The influence of buildings and single trees or groups of trees can be eliminated by filtering of the DSM (PASSINI et al. 2002, DAY et al. 2013), but the effect of filtering forest areas is limited if insufficient ground points are

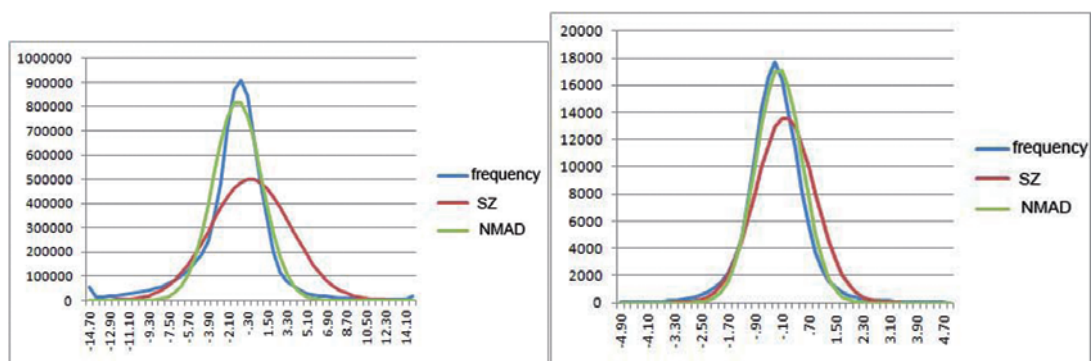


**Fig. 2:** Frequency distribution of discrepancies, left: WorldView-2 DSM against reference DEM, right: WorldView-2 DSM against independent WorldView-2 DSM for open areas.

available. Only by laser scanning in the leaf-off period, or by long wavelength radar, can the ground height be accurately determined in forest areas. Poor image contrast may also be caused by the spectral range of the imager. For example, Cartosat-1 covers the spectral range from  $0.50\ \mu\text{m}$  up to  $0.85\ \mu\text{m}$ , including the near infrared, which provides good contrast in forest regions, while SPOT 5 HRS as well as SPOT 5 are limited to the wavelength range of  $0.48\ \mu\text{m}$  up to  $0.70\ \mu\text{m}$ , which includes little of the infrared range. The histogram for SPOT images is therefore limited to just a few different grey values in forest areas. As an example, a Reference 3D DSM (from SPOT 5 HRS stereo sensor) at the Black Sea region in Turkey, close to the Bulgarian border, needed gap filling by SRTM height values for at least 60% of the area (BÜYÜKSALIH & JACOBSEN 2008) because of matching problems in the forest areas, while a DSM based on a Cartosat-1 stereo pair had only small gaps and these were in areas covered by clouds.

The advantage of pixel-based matching, namely semi-global matching in this case, against area-based matching by least squares is illustrated in Fig.3 (ALOBED et al. 2011). The uneven surface in the lower left corner is caused by trees and the shape of the buildings is better with SGM. On the other hand, the height determined in the centre of the building is approximately the same and the overall accuracy is similar to that from area-based matching. Instead of stereo pairs, tri-stereo models with three images of the same scene

can be employed (TACK et al. 2009). This has advantages in steep mountainous regions and in cities with high buildings where some areas may be occluded in one image, but are present in the other two. Matching is then possible with the nadir and one of the oblique images. In addition, the over-determination of the DHM by three images may improve the accuracy or, more importantly, may lead to better identification of blunders. Of course such blunders may also be determined by filtering and/or manual inspection of the stereo model, which is a process generally required for all height models.

#### 4 Height Models by spaceborne SAR

Height models can be generated by InSAR with an InSAR-configuration having 2 antennas close together, as with the SRTM mission that had a base length of 80 m and a flying elevation of 233 km (BAMLER et al. 2003). The TanDEM-X mission realises its base length by using two SAR satellites in a Helix-configuration (EINER et al. 2013). In the absence of an InSAR-configuration, problems with the phase correlation exist for SAR-image pairs not taken simultaneously, which necessitate a solution by radargrammetry with a much larger base (CAPALDO et al. 2011). InSAR-configurations have the advantage of covering large areas in a short time, as exemplified by the shuttle radar topography mission (SRTM)

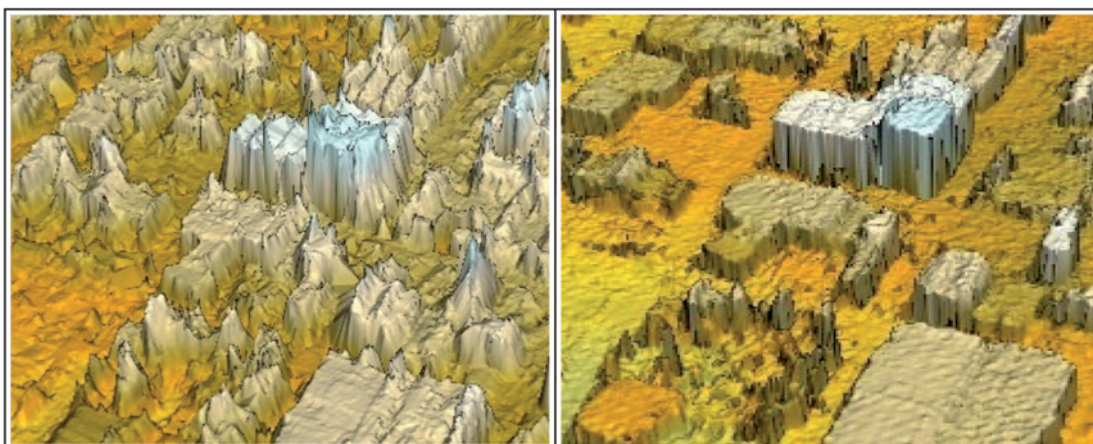


**Fig. 3:** Left: DSM by least squares matching, right: DSM by semi-global matching.

covering the world from 56 °S up to 62.25 °N latitude within 11 days in February 2000. The TanDEM-X-mission will cover the entire world within 2 years, with higher resolution and repeated acquisition from different directions to reduce the influence of radar layover. These missions operate with short wavelength X- and C-band radar which does not penetrate vegetation, so as with optical images, a DSM will be generated.

## 5 Regional to Worldwide Height Models

The generation of height models requires the satellite stereo pair, or tri-stereo pair, along with the matching operation and inspection of the DHM, so it is not free of expense. For this reason, the alternative of using existing height models should be investigated. GMTED 2010, SRTM DSM and ASTER GDEM are height models that are free of charge and readily available. They may well be suitable for a given application, but it may also be economic to use commercial versions of these DHMs. The DHMs are in most cases referenced to geographic coordinates, and corresponding

to this the point spacing is provided in arc-seconds, with 1.0 arcsec at the equator corresponding to 30.9 m. The point spacing and the accuracy are the main criteria for a DHM; the point spacing corresponds to the morphologic details if the DHM has been generated correctly. In the case of the first version of the ASTER GDEM this was not the case. The ASTER GDEM2 is based on stereo models of the ASTER stereo satellite which has a 15 m GSD and all available stereo models were averaged. In the case of the first version of ASTER GDEM the horizontal shifts between the individual DHMs caused by orientation uncertainty were not accounted for and so morphologic details were lost. This was not the case with ASTER GDEM2 available since mid of 2011, and now the morphologic details correspond to the point spacing, as is the case for all the height models listed in Tab. 5.

The accuracy specification for nominally global height models is complex. In Fig. 4 the average of root-mean-square differences for SRTM DHM and ASTER GDEM against a reference DTM is shown. The left-most three columns in the figure show just the root-mean-square height discrepancies. In the case of the centre three columns, RMS height discrepan-

**Tab. 5:** Worldwide and large-area height models.

Height model	Coverage of land area	Spacing	SX, SY	SZ <sub>absolute</sub> <20%	SZ <sub>relative</sub> <20%	Remark
GMTED 2010	100%	7.5 arcsec	Depending upon data source			dominated by SRTM
SRTM	-56° up to 62.25°	3 arcsec	3.5 m – 5 m	6 m – 8 m	4 m	C-band
Aster GDEM2	-83° up to 83°	1 arcsec	10 m	10 m	6 m	15 m GSD, several stereo models
Elevation 30 (SPOT DEM)	43%	1 arcsec	14 m	12 m	6 m	Based on SPOT 5 HRS
Reference 3D	43%	1 arcsec	6 m	5 m	3 m	SPOT DEM improved
NEXMap World 30	100%	1 arcsec	3.5 m – 5 m	5 m	4 m	dominated by SRTM
NEXMap	7%	5 m	1 m	0.6 m – >1.8 m	0.6 m – >1.8 m	airborne-InSAR X-band
TanDEM-X Global DEM	100% available 2014	0.4 arcsec	<4.7 m	<6 m („in meter – range“)	1.2 m	homogenous, actual, DSM later DTM

cies after correction for shifts in X, Y and Z between the respective DSMs and the reference DTM are shown. Note here that following an improved horizontal registration, there is no longer an accuracy difference between ASTER GDEM first version and GDEM2. All height models in Tab. 5 are DSMs with points on top of vegetation and buildings, so a strong influence of the vegetation and buildings is included. If the investigation is limited to open areas, with elimination of remaining non-ground points through filtering, the height discrepancies decrease further, as indicated in the right-hand three columns of Fig. 4. In addition, there is a dependency of the DHM accuracy on terrain inclination, corresponding to the Koppe formula. For open and relatively flat areas, the RMS height difference against the reference DTM for ASTER GDEM is around 6 m, and for SRTM close to 4 m. This is a typical example for the accuracy specification of height models – the influence of the vegetation and the buildings are not reflected via the standard deviation. It is a problem of DHM specification that has to be removed if a DTM is required. In general the accuracy numbers before shift are stated as the absolute accuracy, while after shift they are termed relative accuracy since they are free of the influence of orientation.

Independent of the filtering of model points not belonging to the bare ground, including elimination of blunders, a manual check of the height model, e.g. by 3D-shaded view, should always be made as a part of the quality control process.

The ASTER GDEM depends upon the number of images used for the determination of the individual ground point. This information is provided in a quality file together with the height model. The number of images per point changes depending upon geographic location, and also within a single scene. Based on 12 test areas the relationship  $SZ = 19.1 \text{ m} - 0.72 \cdot (\text{number of images / point})$  has been determined for the ASTER GDEM, and this corresponds to  $SZ = 17.6 \text{ m}$  for 2 images and  $SZ = 3.2 \text{ m}$  for 22 images. This implies that the accuracy of ASTER GDEM is not as homogenous as the SRTM DSM. Nevertheless, in spite of the lower accuracy, it has the advantage of better morphologic details with its 1 arcsec point spacing. By this reason, Intermap generated the NextMap World30 DEM as a fusion of the SRTM DSM and ASTER GDEM, with improved absolute location accuracy via registration with height profile points from ICESat. In addition to the SRTM C-band data from the USA, the German-Italian SRTM X-band data are available with 1arcsec point spacing, but the area coverage is less than for the SRTM C-band height data. Elevation 30 and Reference 3D are based on the SPOT 5 HRS stereo sensor. They are currently available for approximately 43% of the Earth's landmass, though stereo scenes cover most parts of the world. Additional height models can be generated by ASTRIUM upon request. Reference 3D was improved by post-processing for better orientation and for elimination of blunders. Gaps, especially in forest areas, have been filled in most cases by SRTM data, with

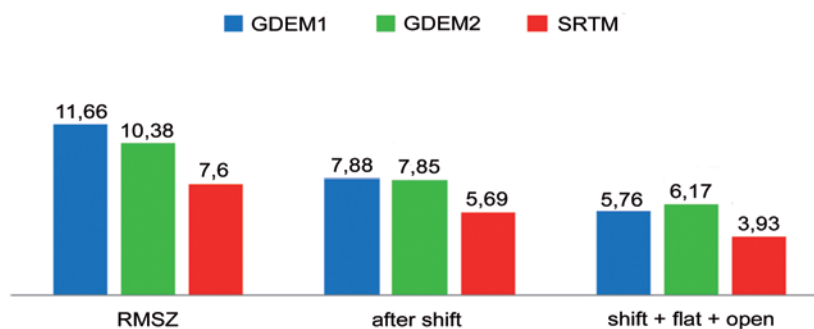


**Fig. 4:** RMS height discrepancies of SRTM and ASTER GDEM against reference height models, as averaged over 12 test areas distributed worldwide.

gaps in the SRTM DSM having often been filled with SPOT 5 HRS data.

NextMap, based on aerial InSAR, is available for West-Europe, large parts of the USA, and areas in Indonesia and Australia. The accuracy is strongly dependent upon radar lay-over, so it has a stronger accuracy variation, between  $SZ = 0.6$  m and  $SZ > 1.8$  m. A major change for worldwide height models will come in 2014 with the release of the TanDEM-X Global DEM. A large part of the data acquisition has always been completed. The Basic version without manual checking for blunders will be initially available. This will be followed by the checked DSM-version and later a DTM-version. The relative accuracy is specified as a standard deviation of 1.2 m within a  $1^\circ \times 1^\circ$  scene ( $111^2$  km<sup>2</sup> at the equator). Originally, the absolute standard deviation for the height was specified as 6 m, but according to EINEDER et al. (2013), accuracy will be in the “metre range” due orientation refinements determined from ICESat and sea level heights. Together with this hitherto unobtainable high accuracy and 0.4 arcsec grid spacing (12 m at the equator) for large-area height models, TanDEM-X DEM will be clearly better than all other DHMs with the exception of height models from very high resolution optical satellites, but they cannot cover very large regions.

## 6 Conclusion

The determination of height models based on space images now overlaps in accuracy and resolution with determinations based on aerial images. Space images have the advantage of global coverage and global access. With very high resolution optical satellite images, available with up to 0.5 m GSD, a system accuracy of approximately 0.5 m standard deviation for the height can be reached for vegetation-free areas with good contrast. A height model usually includes parts with suboptimal contrast and the influence of vegetation and buildings, so the accuracy of the DTM is generally not as good. Similar problems exist with InSAR using short X- or C-band wavelengths. The influence of vegetation and buildings can be reduced by filtering and additional manual in-

spection, but in forest areas with not enough points on the solid ground, filtering from DSM to DEM is limited. Independent of the lower accuracy for steeper terrain, the comparison of a DHM with a reference DEM will show in most cases larger height discrepancies than might be anticipated within a normal distribution. This is due to the influence of remaining vegetation and buildings, along with areas exhibiting problems of image matching or radar overlay. The NMAD better describes the frequency distribution of the majority of height differences than the standard deviation, but it should be anticipated that larger discrepancies will occur. Only by filtering, together with final manual revision, can the percentage of larger height errors be reduced. Nevertheless, a high level of accuracy and resolution can today be reached by DEM-determination from space images, indeed the accuracy is invariably higher than the national DEMs produced in several countries by their survey administrations. With the TanDEM-X Global DEM, a new level of worldwide height modeling accuracy will be reached. With VHR optical space images even better accuracy and resolution are possible, but worldwide coverage via VHR stereo models is today not economically feasible, so only local and regional DHMs from such imagery can be anticipated for the foreseeable future. In instances where highest accuracy and resolution are not required, existing readily available large-area DHMs should not be overlooked.

## References

- ALOBED, A., JACOBSEN, K., HEIPKE, C. & ALRAJHI, M., 2011: Building Monitoring with Differential DSMs. – ISPRS Hannover Workshop 2011, International Archives of Photogrammetry and Remote Sensing **XXXVIII-4/W19**.
- BAMLER, R., EINEDER, M., KAMPES, B., RUNGE, H. & ADAM, N., 2003: SRTM and beyond: current situation and new developments in spaceborne InSAR. – Hannover Workshop 2003, <http://www.ipi.uni-hannover.de/fileadmin/institut/pdf/bamler.pdf> (3.7.2013).
- BÜYÜKSALIH, G. & JACOBSEN, K. 2008: Digital Height Models in Mountainous Regions based on Space Information. – EARSel Workshop Remote Sensing – New Challenges of High Resolution, Bochum 2008.

- CAPALDO, P., CRESPI, M., FRATARCANGELI, F., NASCETTI, A. & PIERALICE, F., 2011: DSM generation from high resolution COSMO-SKYMED imagery with radargrammetric model. – Hannover Workshop, International Archives of Photogrammetry and Remote Sensing Vol **XXXVIII-4/W19**.
- DAY, D., JACOBSEN, K., PASSINI, R. & QUILLEN, S., 2013: A Study on Accuracy and Fidelity of Terrain Reconstruction after Filtering DSMs produced by Aerial Images and Airborne LiDAR Surveys. – ASPRS Annual Convention 2013, Baltimore, MD, USA.
- EINER, M., BAMLER, R., CONG, X., GERNHARDT, S., FRITZ, T., ZHU, X., BALSS, U., BREIT, H., ADAM, N. & FLORICIOIU, D., 2013: Globale Kartierung und lokale Deformationsmessungen mit den Satelliten TerraSAR-X und TanDEM-X. – Zeitschrift für Vermessungswesen **1/2013**: 75–94.
- HIRSCHMÜLLER, H., 2005: Accurate and Efficient Stereo Processing by Semi-Global Matching and Mutual Information. – IEEE Conference on Computer Vision and Pattern Recognition, CVPR'05 **2**: 807–814, San Diego, CA, USA.
- PASSINI, R., BETZNER, D. & JACOBSEN, K., 2002: Filtering of Digital Elevation Models. – ASPRS annual convention 2002, Washington D.C., USA.
- TACK, F., GOOSSENS, R. & BÜYÜKSALIH, G., 2009: Semi-automatic city model extraction from tri-stereoscopic vhr satellite imagery. – International Archives of Photogrammetry and Remote Sensing XXXVIII-3/W4.

## Address of the Author:

Dr.-Ing. KARSTEN JACOBSEN, Leibniz Universität Hannover, Institut für Photogrammetrie und Geoinformation, D-30167 Hannover, Nienburger Str. 1, Tel.: +49-511-762-2485, Fax: +49-511-62-2483, e-mail: jacobsen@ipi.uni-hannover.de

Manuskript eingereicht: April 2013

Angenommen: Juni 2013